Chemical Science

ROYAL SOCIETY OF CHEMISTRY

EDGE ARTICLE

View Article Online
View Journal

Cite this: DOI: 10.1039/d6sc01392a

All publication charges for this article have been paid for by the Royal Society of Chemistry

Mastering the potential of well-defined ML^1L^2 species in asymmetric catalysis through ligand immobilization ($ML^{het}L^{hom}$). Use in highly enantioselective Pd-catalyzed spiroannulation

Maria Biosca,†[a] Pol de la Cruz-Sánchez, †[a] Jorge Faiges,†[a] Aitor Maestro,[bc] C. Oliver Kappe, [bc] Sándor B. Ötvös, *[bc] Miquel A. Pericàs, [ad] Oscar Pàmies[a] and Montserrat Diéguez *[a]

Catalytic complexes involving different monodentate ligands coordinated to the same metal center offer considerable interest towards the development of new processes and the improvement of the characteristics of known ones. However, one of the major drawbacks in using mixtures of monodentate ligands in asymmetric metal catalysis lies in the difficulty of controlling the formation of active species containing both of the desired ligands coordinated at the same time to the metal center (ML^1L^2). Herein, we present a straightforward methodology to overcome this long-standing major limitation. Thus, we demonstrate that the formation of well-defined ML^1L^2 species can be attained by combining an immobilized ligand and a homogeneous ligand. This concept has been successfully applied to a synthetically relevant Pd-catalyzed [3 + 2] spiroannulation. The use of a polystyrene supported chiral binaphthyl-based phosphoramidite in combination with an achiral cheap biphenyl monophosphoramidite led to the sole formation of highly enantioselective active species containing both ligands coordinated to Pd, as demonstrated by gel-phase, high resolution ^{31}P NMR. In addition, we have also studied the continuous flow spiroannulation, which further demonstrated that the reaction occurs in the heterogenous phase. The advantages associated to the use of well-defined $PdL^{het}L^{hom}$ in catalysis are further demonstrated in asymmetric allylic alkylation reactions, illustrating the potential of this methodology in asymmetric catalysis.

Received 16th February 2026
Accepted 8th May 2026

DOI: 10.1039/d6sc01392a

rsc.li/chemical-science

Introduction

Enantioselective metal catalysis has become pivotal in the synthesis of enantiomerically enriched compounds. Its success mainly relies on the use of chiral ligands able to transfer the chiral information from the catalysts to the product.[1–3] In this realm, there are many relevant transformations whose enantiodetermining transition states involve two monodentated ligands (or a bidentate one) coordinated to the metal. The successful introduction of DIOP[4] in the early 70's favored the use of chiral bidentate ligands instead of monodentate ligands. However, the development of DuPHOS-type monophospholane[5] and binol-based mono-phosphonite,[6,7] phosphite[8] and phosphoramidite[9,10] ligands in the late 90's and early 2000's paved the way for the use of monodentate ligands in asymmetric catalysis, outperforming bidentate ligands in certain cases. Nowadays, many reactions depend on them for excellent catalytic performance.[1–3,11] Soon after, Reetz and coworkers went a step further by employing mixtures of chiral monodentate ligands (L^1 and L^2), thereby introducing a new concept in asymmetric catalysis that mimics the desymmetrization of C_2-symmetric bidentate ligands into their C_1-symmetric counterparts.[12,13] An inherent limitation of this approach arises from the presence of three distinct catalytically active species in equilibrium: the two homocombinations (ML^1L^1 and ML^2L^2) and the desired heterocombination ML^1L^2 (Fig. 1a(1)). Using a combinatorial approach, Reetz and coworkers identified certain ligand heterocombinations that were more reactive and, in some cases, more enantioselective than the two possible homocombinations in Rh-catalyzed hydrogenation (Fig. 1a(1)). These findings are consistent with reports showing that certain C_1-symmetric P–P′ bidentate ligands can outperform their C_2-symmetric analogues.[13] They

[a]Universitat Rovira i Virgili, Departament de Química Física i Inorgànica, C/ Marcel lí Domingo, 1, 43007 Tarragona, Spain. E-mail: montserrat.dieguez@urv.cat
[b]Institute of Chemistry, University of Graz, NAWI Graz, A-8010 Graz, Austria
[c]Center for Continuous Flow Synthesis and Processing (CC FLOW), Research Center Pharmaceutical Engineering GmbH (RCPE), A-8010 Graz, Austria. E-mail: sandor.oetvoes@rcpe.at
[d]Royal Academy of Sciences and Arts of Barcelona, Chemistry Section, La Rambla 115, 08002 Barcelona, Spain
† These authors contributed equally, and they are arranged alphabetically.

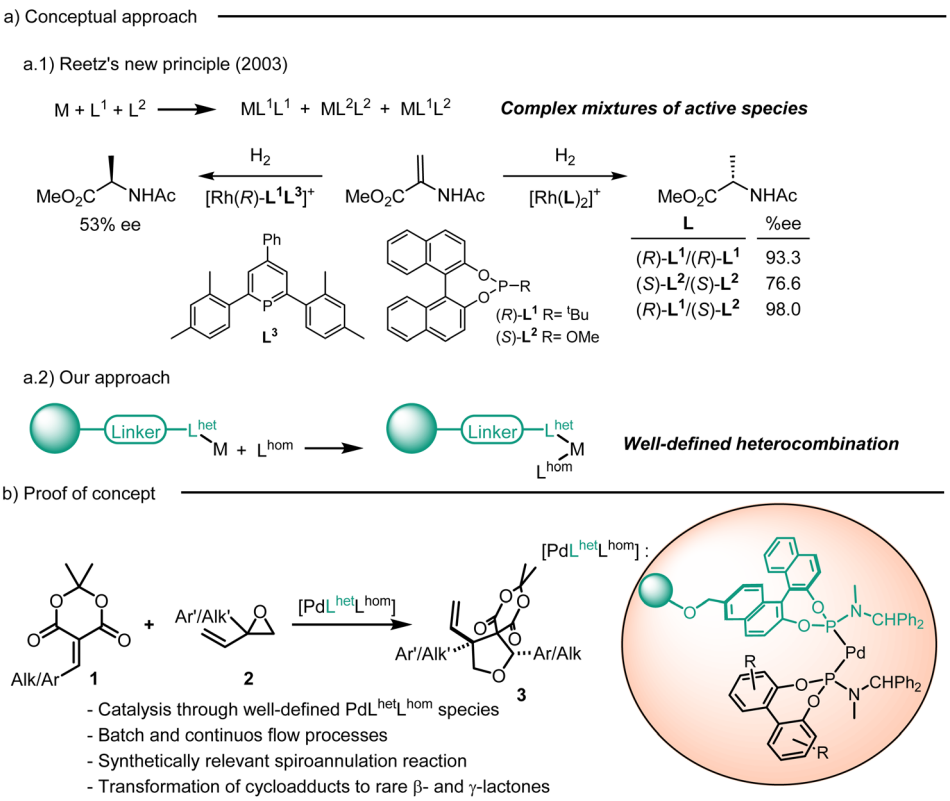

Fig. 1 (a) Conceptual approach in the search of well-defined active species containing two distinct monodentate ligands (heterocombination); and (b) enantioselective spiroannulation towards structurally complex tetrahydrofuran-fused spirocyclic scaffolds as proof of concept.

further demonstrated that the sense of enantioselectivity can be reversed by selecting an appropriate mixture of chiral and achiral monodentate ligands (Fig. 1a(1)).[14] However, the broader application of this strategy in asymmetric catalysis has been limited by the coexistence of multiple catalytically active species, the sensitivity of their equilibria to changes in reaction conditions and substrate, and the requirement that the heterocombination must be both more reactive and selective than the corresponding homocombinations to provide an improved catalytic system.[15] Accordingly, since its first report in 2003, this approach has been explored in relatively few occasions, mainly within a relatively short time frame (2003–2008), and predominantly in asymmetric hydrogenation, with limited success in other asymmetric transformations.[15]

Based on our experience in covalent ligand immobilization[16,17] as well as in the effective site isolation of immobilized ligands onto organic[18,19] or inorganic[20] supports, which prevents the coordination of two such immobilized ligands to a single metal atom, we envisaged exploring catalytic systems involving two different monodentate ligands in which one ligand remains in solution while the other is appropriately immobilized onto a solid support (Fig. 1a(2)). Whenever the condition of site isolation is fulfilled in the immobilized ligand, this should lead to the exclusive formation of a perfectly defined immobilized heterodimeric species $ML^{Het}L^{Hom}$. It is worth noting that, since the liquid phase in these systems can be simply washed away by filtration, it should be possible to remove any excess of the homogeneous ligand prior to the catalytic use. Moreover, since a two-phase system is involved, the generation in the liquid phase of $ML^{Hom}L^{Hom}$ species would only be possible subsequently to non-favorable metal leaching. Moreover, the exclusive formation of $ML^{Het}L^{Hom}$ species would easily pave the way towards the implementation of a heterogenized continuous flow protocol, with its concomitant advantages with respect to the still more common batch processing.[21,22]

To bring these ideas into practice, we hypothesized that ML^1L^2 species of the $ML^{Het}L^{Hom}$ type would be easily and selectively accessed by first coordinating the metal center from a convenient precursor to an immobilized ligand (L^{het}) followed by the addition of the second, homogeneous ligand (L^{hom}) in solution and washing away any excess of it if necessary (Fig. 1a(2)). To avoid leaching of the valuable immobilized ligand, we selected a covalent immobilization strategy, while to preserve the selectivity characteristics of the parent homogeneous ligand we placed the immobilization point far away from the catalyst chiral pocket to avoid perturbation of the enantiodetermining transition states. As a support, we selected a Merrifield-type polystyrene (PS) resin with low cross-linking and low functionalization. This support offered several advantages. Firstly, the resulting resins swells efficiently in most common organic solvents and can therefore be easily characterized using standard NMR techniques, while providing a homogeneous-like environment for the catalytic process. In addition, the low

functionalization of the resulting catalytic resins allows strict site isolation, so that no homocombination of ligands ($ML^{Het}L^{Het}$) is possible due to geometrical constraints.

To test our hypothesis, we selected the enantioselective Pd-catalyzed [3 + 2] spiroannulation and evaluated it under two scenarios: the usual batch process and in continuous flow, by taking advantage in both cases of the exclusive formation of well-defined $PdL^{Het}L^{Hom}$ active species (Fig. 1b). The reaction was chosen because its active species usually involves two monodentate ligands coordinated to Pd[23–36] and because of the increasing interest of spirocyclic motifs which are present in many natural products, drugs and functional materials.[37–42] In particular, we selected the reaction of 2-substituted-2-vinylepoxides with 5-benzylidene Meldrum's acid derivatives leading to spirocyclic tetrahydrofuran derivatives which remains comparatively underexplored.[43] To further illustrate the synthetic value of this particular process, we straightforwardly converted one of the enantiopure spirocyclic products into rare and highly appealing enantiopure lactone motifs, which include enantiopure spirocyclic-β-, fused bicyclic γ- and α-benzylidene γ-lactones.

Results and discussion

Development of the spiroannulation reaction under homogeneous conditions using monodentate ligands

Catalyst search and mechanistic studies. A remarkable subclass of spirocycles is that including a tetrahydrofuran ring, such scaffold being present in many natural products and synthetic drugs.[44–50] Although Pd [3 + 2] cycloaddition reactions have emerged as an atom economical alternative to forge tetrahydrofuran-fused spirocyclic scaffolds, since the first report in 2016 there are very few reports dealing with this subject,[51–55] and these are mainly limited to the synthesis of oxindole-containing spirocyclic tetrahydrofuran compounds, which are obtained with broadly varying selectivities.[53–55] We reasoned that this reaction would represent an optimal conceptual laboratory for the study of the catalytic use of $PdL^{Het}L^{Hom}$ ligands and decided to perform it by using Meldrum acid derivatives as Michael acceptors and vinyl-epoxides as π-allylpalladium precursors. This could lead to spirocyclic tetrahydrofuran-fused derivatives, a structural class including compounds with a wide range of biological activities[56–58] and presenting remarkable synthetic potential (see SI for derivatization experiments). To study the viability of our approach, we selected the reaction of 5-(4-methoxybenzylidene)-2,2-dimethyl-1,3-dioxane-4,6-dione (**1a**) with 2-phenyl-2-vinyloxirane (**2a**) using $Pd_2dba_3\cdot CHCl_3$ as catalyst precursor (Table 1). Both reaction partners provide an appealing platform for preparing new tetrahydrofuran-fused spirocyclic derivatives thanks to the range of substituents (R^1 and R^2) that could be attached to them (*vide infra* Scheme 3). We focused on evaluating a range of monodentate monophosphoramidite ligands and benchmarking them over other typically used bidentate ligands in asymmetric π-allyl Pd catalysis (see SI). In this manner, we found that the use of monophosphoramidite $\mathbf{L_1}$ outperforms the commonly used bidentate ligands, exclusively affording the sole formation of [3 + 2]-cycloadducts (Table 1, entry 1). Solvent examination showed that the use of THF provided somewhat better results, especially in terms of diastereoselectivity (entries 1–4). Decreasing the temperature had a deleterious effect on activity and diastereoselectivity (entry 5). We then focused on studying the effect of the ligand parameters by varying the amino moiety in $\mathbf{L_1}$ (with ligands $\mathbf{L_2}$–$\mathbf{L_6}$; entries 6–10) and by varying the chiral backbone (with related spirocyclic-based ligands $\mathbf{L_7}$–$\mathbf{L_9}$; entries 11–13). We found that binaphthyl-based ligand $\mathbf{L_5}$ boosted the enantioselectivity to >99% ee (entry 9). Although the use of $\mathbf{L_5}$ yielded the diastereomeric [3 + 2]-cycloaddition products **3aa** and **3′aa** in a modest 3 : 1 ratio, the major diastereoisomer **3aa** could be easily secured in pure form by crystallization through simple addition of isopropyl alcohol to a concentrated dichloromethane solution of the crude reaction product. Thus, by taking advantage of this feature we could secure **3aa** in good isolated yield (73%) and in excellent diastereo- and enantiopurity (entry 14) working at room temperature. Moreover, the reaction can be carried out in environmentally friendly solvents, such as 2-MeTHF, with no loss of selectivity.

To verify that the species responsible for the catalytic activity contains two monodentate ligands coordinated to Pd through the catalytic cycle, we performed mechanistic investigations, including kinetic and NMR studies and Eyring plot analysis. We initially performed kinetic studies using the variable time normalization analysis (VTNA).[59–61] To facilitate data collection by ^{19}F-NMR, we chose the reaction of 5-(4-trifluorobenzylidene)-2,2-dimethyl-1,3-dioxane-4,6-dione (**1b**) with 2-phenyl-2-vinyloxirane (**2a**) leading to spirocyclic furan **3ba**. We first determined the rate dependence on Meldrum's acid-type derivative (**1b**) and epoxide (**2a**) concentration. As shown in Fig. 2, a first-order dependence in **2a** was determined, which indicates that this species participates in the rate-determining step of the reaction.

In contrast, the reaction exhibited a negative order in Meldrum's acid-type derivative concentration ([**1b**]), indicating that **1b** acts as an inhibitor. Accordingly, the presence of Pd species containing coordinated **1b** were observed during the kinetic experiments in the ^{19}F-NMR spectra as a broad signal at a −62.5 ppm (see SI).

We then determined the reaction order in catalyst and found a value higher than one (see SI), which is consistent with the off-cycle formation of catalytically inactive dimeric species containing coordinated **1b**.[62] In addition, the presence of free ligand was not observed in any of the $^{31}P\{^1H\}$ NMR spectra recorded at different stages of the catalytic reaction (see SI), which indicates that the two monophosphoramidite ligands remain coordinated to palladium through all the catalytic cycle.

Overall, our experimental data support a mechanism where coordination of multiple molecules of **1b** originates off-cycle dimeric palladium species **A** that is in equilibrium with a monomeric Pd-active species **B** containing two coordinated monophosphoramidites (Scheme 1).

As already mentioned, no free ligand was observed by $^{31}P\{^1H\}$-MMR spectroscopy during the course of the reaction. Rate-determining step coordination of the vinyloxirane to the

Table 1 Pd-catalyzed cycloaddition of **1a** and **2a** with ligands L_1–L_9[a]

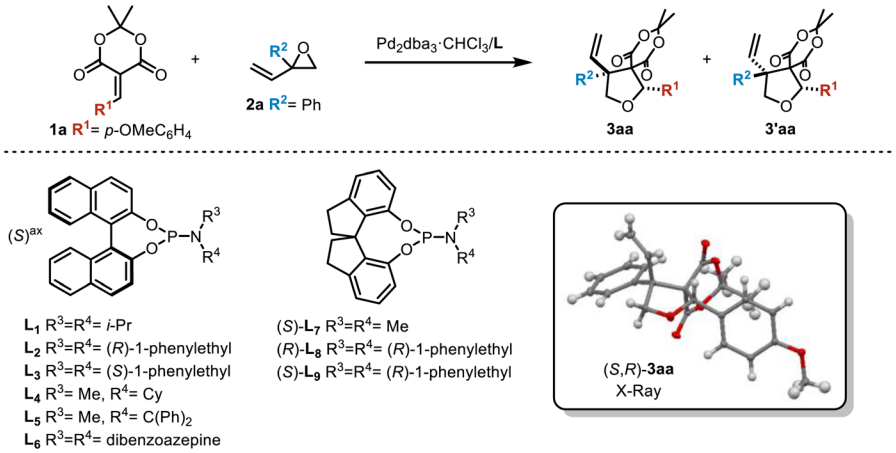

Entry	Ligand	Solvent	T (°C)	% Conv[b]	% Yield[c]	**3aa** : **3′aa**[b]	%ee[d]
1	L_1	THF	25	100	98	8 : 1	93 (*S*,*R*)
2	L_1	CH_3CN	25	99	95	7 : 1	92 (*S*,*R*)
3	L_1	CH_2Cl_2	25	95	93	4 : 1	91 (*S*,*R*)
4	L_1	Toluene	25	98	91	7 : 1	93 (*S*,*R*)
5	L_1	THF	0	21	14	3 : 1	91 (*S*,*R*)
6	L_2	THF	25	<5	—	—	—
7	L_3	THF	25	27	19	1 : 1	22 (*S*,*R*)
8	L_4	THF	25	100	97	7 : 1	91 (*S*,*R*)
9	L_5	THF	25	100	>99	3 : 1	>99 (*S*,*R*)
10	L_6	THF	25	100	>99	3 : 1	90 (*S*,*R*)
11	L_7	THF	25	100	>99	6 : 1	33 (*S*,*R*)
12	L_8	THF	25	100	99	4 : 1	30 (*S*,*R*)
13	L_9	THF	25	50	49	2 : 1	63 (*S*,*R*)
14[e]	L_5	THF	25	100	73[f]	>20 : 1[f]	>99 (*S*,*R*)

[a] Reaction conditions: $Pd_2(dba)_3 \cdot CHCl_3$ (2.5 mol%), ligand (10 mol%), **1a** (0.1 mmol), **2a** (0.2 mmol), solvent (1.0 mL), 25 °C, overnight. [b] Measured by ^{1}H-NMR. [c] Isolated yields as a mixture of diastereomers. [d] Referred to the major diastereomer and determined by HPLC using a chiral stationary phase. [e] Reaction carried out at 2 mmol scale. [f] After recrystallization. X-ray structure of enantiopure (*S*,*R*)-**3aa** is also shown.

intermediate **B** is followed by oxidative addition to form the key zwitterionic Pd–allyl complex with two coordinated chiral monophosphoramidite ligands (**C**). Nucleophilic attack of the Pd–zwitterionic species on **1b**, followed cyclization, leads to the formation of **3ba** while closing the catalytic cycle.

We next calculated the activation parameters using the Eyring equations.[63] Based on the Eyring plot (Fig. 3), we calculated the following values: $\Delta H^{\ddagger} = 18.0 \pm 2$ kcal mol^{-1}; $\Delta S^{\ddagger} = -16.5 \pm 8$ cal mol^{-1} K^{-1}; $\Delta G^{\ddagger} = 23.0 \pm 5$ kcal mol^{-1}. The negative value of $\Delta S^{\ddagger}$ indicates that entropy decreases on forming the transition state, which is consistent with coordination of the vinyloxirane as the rate determining step.

Development of well-defined PdL^1L^2 species by combining an immobilized ligand and a homogeneous ligand

Application in batch and scope of the reaction. Once confirmed that in the active species of the new spiroannulation reaction two monodentate phosphoramidites are coordinated

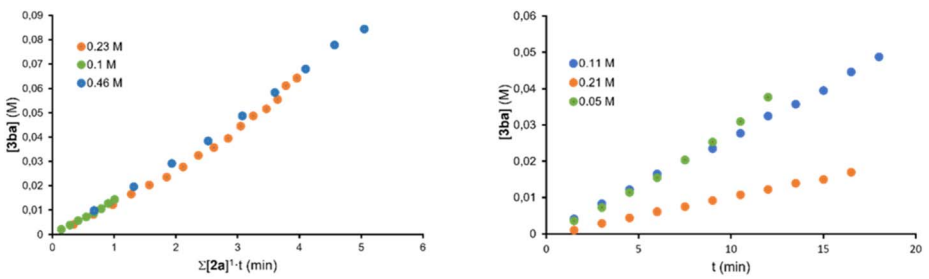

Fig. 2 Kinetic study of order in **2a** (left) and **1b** (right).

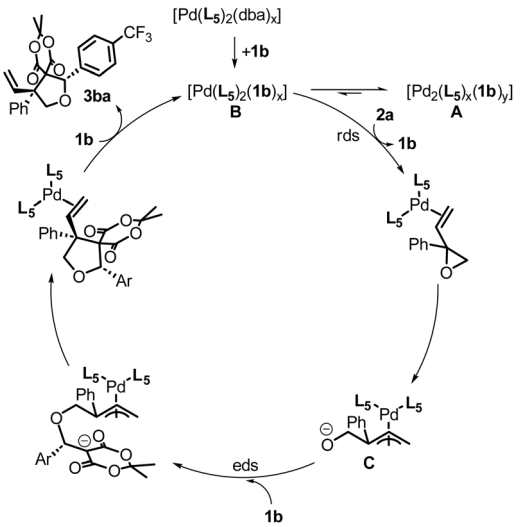

Scheme 1 Mechanistic proposal for the [3 + 2]-cycloaddition for the preparation of tetrahydrofuran-fused spirocyclic Meldrum's acid derivatives using Pd(*S*)-L_5 catalytic system (Ar = *p*-CF_3-C_6H_4). Rds = rate determining step. Eds = enantiodetermining step.

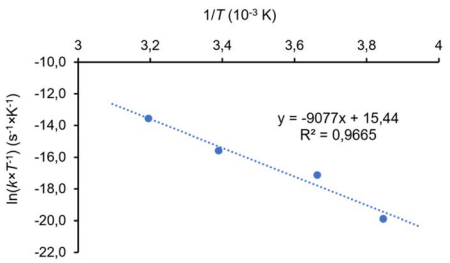

Fig. 3 Eyring plot for the [3 + 2]-cycloaddition of **1b** and **2a** with PdL_5 catalytic system.

to Pd, we proceeded to immobilize the best ligand found in the initial screening (*R*)-$\mathbf{L_5}$ onto Merrifield resin with low crosslinking (1% DVB) and low functionalization (f = 0.6 mmol g^{-1}). The low crosslinking is key to ensure a good swelling of the resin providing a homogeneous-like environment, while the low functionalization facilitates catalytic site isolation. The immobilization started with the synthesis of the PS-supported (*R*)-binol **4** (Scheme 2), by covalently linking the resin to the ligand through a carbon atom far away from the catalytic center to ensure that the catalyst could have a selectivity comparable to its homogeneous counterpart.

Following the methodology reported by the Sasai group,[64] PS-(*R*)-**4** was easily prepared in three-steps from (*R*)-6-bromo-2,2′-bis(ethoxymethoxy)-1,1′-binaphthalene (*R*)-**5**. With only one more step, PS-(*R*)-**4** was then transformed into the desired immobilized phosphoramidite PS-(*R*)-$\mathbf{L_5}$ by reaction with PCl_3 followed by reaction with *N*-methyl-1,1-diphenylmethanamine. The catalytic resin PS-(*R*)-$\mathbf{L_5}$ was obtained with a functionalization of f = 0.41 mmol according to the elemental analysis of nitrogen. This corresponds to an immobilization yield of 89%.[65]

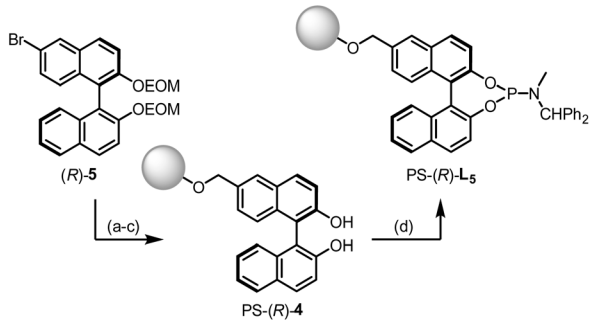

Scheme 2 Synthesis of PS-(*R*)-L_5. Reaction conditions: (a) DMF, THF, −50 °C, 3 h then $NaBH_4$, MeOH, 0 °C, 3 h; (b) NaH, THF, Merrifield resin, rt, 16 h; (c) HCl (aq), THF, rt; (d) PCl_3, Py, 90 °C, 16 h, then *N*-methyl-1,1-diphenylmethanamine, NEt_3, DMAP, toluene, rt, 5 h (OEM = ethoxymethyl).

The performance of PS-(*R*)-$\mathbf{L_5}$ was initially studied in the model cycloaddition reaction of **1a** with **2a** under batch conditions (Table 2, entry 1), delivering **3aa** in racemic form. This is a highly positive result because it confirms that the physical separation between the ligands on the resin satisfies the site isolation requirement, so that $PdL^{Het}L^{Het}$-type species cannot be generated, which is essential for our approach to succeed. To further confirm this interpretation, we added one equivalent of homogeneous (*R*)-$\mathbf{L_5}$, which resulted in a remarkable recovery of enantioselectivity (85% ee, entry 2). This finding agrees with the mechanistic investigations that show that two phosphoramidite units [PS-(*R*)-$\mathbf{L_5}$ and (*R*)-$\mathbf{L_5}$] are involved in the lowest energy, enantiodiscriminating transition state. As a further confirmation that the addition of monomer (*R*)-$\mathbf{L_5}$ is not simply promoting the spiroannulation in solution, the addition of the same amount of (*S*)-$\mathbf{L_5}$ led to a much lower enantioselectivity

Table 2 Spiroannulation using different ligand combinations in homogeneous and heterogeneous phases[a]

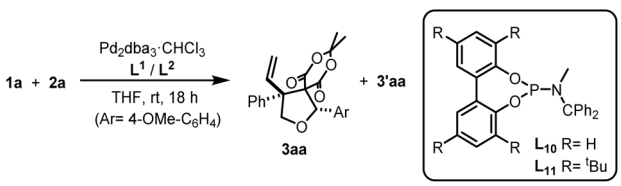

Entry	L^1	L^2	% Conv[b]	**3aa : 3′aa**[b]	%ee[c]
1	PS-(*R*)-$\mathbf{L_5}$	—	100	2.7 : 1	0
2	PS-(*R*)-$\mathbf{L_5}$	(*R*)-$\mathbf{L_5}$	100	3 : 1	85 (*R*,*S*)
3	PS-(*R*)-$\mathbf{L_5}$	(*S*)-$\mathbf{L_5}$	54	3 : 1	33 (*R*,*S*)
4	PS-(*R*)-$\mathbf{L_5}$	$\mathbf{L_{10}}$	60	3 : 1	82 (*R*,*S*)
5	**PS-(*R*)-$\mathbf{L_5}$**	$\mathbf{L_{11}}$	**100**	**3 : 1**	**95 (*R*,*S*)**
6	(*S*)-$\mathbf{L_5}$	$\mathbf{L_{10}}$	46	3 : 1	7 (*S*,*R*)
7	**(*S*)-$\mathbf{L_5}$**	$\mathbf{L_{11}}$	**76**	**3 : 1**	**50 (*S*,*R*)**

[a] Reaction conditions: $Pd_2(dba)_3 \cdot CHCl_3$ (2.5 mol%), ligand (5 mol% of each ligand), **1a** (0.1 mmol), **2a** (0.2 mmol), THF (1.0 mL), 25 °C, overnight. [b] Conversions and diastereomeric ratios determined by ^{1}H-NMR. [c] Enantiomeric excesses determined by HPLC.

(33% ee; entry 3), pointing to the operation of a mismatched ligand combination.

The results obtained so far clearly indicate that it is possible to generate well-defined $PdL^{Het}L^{Hom}$ species, opening the possibility to optimize the catalytic outcome by selecting the appropriate homogeneous ligand (L^{Hom}). For that purpose, we generated two different $PdL^{Het}L^{Hom}$ species by mixing PS-(*R*)-**L$_5$** with achiral ligands **L$_{10}$** or **L$_{11}$**, which differ in the bulkiness of the biphenyl moiety. The use of species involving the less sterically congested ligand **L$_{10}$** (Pd(PS-(*R*)-**L$_5$**)**L$_{10}$**) led to a moderate conversion but a promising enantioselectivity (82% ee, entry 4). We were delighted to see that the use in the mixed species of the bulkier ligand **L$_{11}$** boosted the enantioselectivity to 95% ee (entry 5), with a complete conversion. This proves that under our conditions the formation of the heterocombination Pd(PS-(*R*)-**L$_5$**)**L$_{11}$** is not only preferred over the homocombination (Pd**L$_{11}$L$_{11}$**), but also it is highly enantioselective (entry 5 *vs.* 7). We further proved the formation of Pd(PS-(*R*)-**L$_5$**)**L$_{11}$** species by performing a sol–gel $^{31}P\{^1H\}$ NMR of an equimolar mixture of supported PS-(*R*)-**L$_5$** and **L$_{11}$** that upon addition of $Pd_2(dba)_3$ showed the complete disappearance of the sharp signal corresponding to monomeric **L$_{11}$** and its rapid incorporation into the broad ^{31}P band of the polymer-supported monophosphoramidite ligand (see SI). Moreover, the results obtained using Pd(PS-(*R*)-**L$_5$**)**L$_{10}$** and Pd(PS-(*R*)-**L$_5$**)**L$_{11}$** indicate that the tropoisomerism of the biphenyl moiety in inexpensive ligands **L$_{10}$** and **L$_{11}$** is efficiently controlled by a nearby chiral moiety – in our case, PS-(*R*)-**L$_5$**.[66] Accordingly, the results indicate that in both **L$_{10}$** and **L$_{11}$**, the biphenyl moiety adopts an (*R*)-configuration in the active Pd species.[67]

In line with the spectroscopic evidence, the combination of equimolecular amounts of ligand (*S*)-**L$_5$** with achiral **L$_{11}$** under homogeneous conditions (Table 2, entry 7) led to much lower conversion and enantioselectivity than when using the Pd(PS-(*R*)-**L$_5$**)**L$_{11}$** species (entry 5): 50 *vs.* 95% ee. The same behaviour is observed for the combinations involving **L$_{10}$** (entries 4 and 6). These results agree with the formation in solution of a mixture of active species containing both homodonor combinations and possibly the heterocombination, further confirming the difficulty of controlling the speciation of the active species in homogeneous phase.

We subsequently studied the scope of the reaction catalyzed by Pd(PS-(*R*)-**L$_5$**)**L$_{11}$**. Positively, the use of a range of 5-benzylidene Meldrum's acid derivatives (**1a–l**) and 2-aryl-2-vinyloxiranes (**2a–j**) led to the formation of the corresponding tetrahydrofurans in high yields and high-to-excellent enantioselectivities (Scheme 3), mean ee's 95.2%; 24 examples in total) regardless of the aryl substitution pattern and the electronic properties of the aryl substituents at both coupling units. The diastereoselectivities were affected by the substitution of the aryl group at the Meldrum's acid derivative, with the lowest diastereoselectivity observed when an electron withdrawing *p*-CF_3 group was present, while the existence of substituents at the *ortho* position had a very positive impact on the diastereoselectivity, allowing to reach dr's (up to >20 : 1) without the need of further crystallization, see products **3gd**, **3gf**, **3gi**). Notably, the reaction also tolerated well the presence of heteroarylmethylidene substituted (**3ia** and **3ja**) and conjugated alkylidene Meldrum's acid derivatives (**3la**). Finally, the spiroannulation of Meldrum's acid derivatives with aliphatic substituents as well as with 2-alkyl-2-vinyloxiranes proceeded also well to form the corresponding tetrahydrofurans **3ka** and **3bj** in high yields and enantioselectivities (95–96% ee).

Noteworthy, diastereomerically pure **3aa** could be converted in a straightforward manner into enantiopure spirocyclic-β-, fused bicyclic γ- and α-benzylidene γ-lactones (see SI for details).

Recycling experiments in batch and toward continuous flow using well determined heterodonor Pd(PS-(*R*)-L$_5$)L$_{11}$ species

The heterogeneous nature of the catalytic system prompted us to study the possibility of catalyst recycling. Our first attempts were directed to the recovery of the catalyst by filtration and its reuse in batch. However, all our attempts in this direction failed. This was probably linked to the formation of inactive palladium black species, which was observed during work-up of every single catalytic experiment. This was not unexpected, since the formation of Pd black is typically reported after the use of palladium complexes in homogeneous catalysis. We then focused on the development of a more sustainable version of the annulation reaction, by developing a continuous flow version of the process in which separation and recycling of the heterogenized catalyst are integrated into the same process and would not require the breakdown of inert atmosphere, anhydrous conditions.

For this purpose, a packed bed reactor was assembled by placing PS-(*R*)-**L$_5$** (0.25 g, 0.1 mmol) in a size-adjustable glass column. After swelling the resin with THF, the reactor was flushed with a stock solution of $Pd_2(dba)_3 \cdot CHCl_3$ (6 mM in THF) for 20 minutes (0.2 mL min^{-1}, 0.024 mmol). Then, a THF solution containing the second achiral ligand **L$_{11}$** was pumped for 20 minutes to generate *in situ* the active Pd complex (0.2 mL min^{-1}, 0.05 mmol). Finally, a THF solution of **1a** and **2a** ([**1a**] = 0.025 M, [**2a**] = 0.033 M) was pumped at 0.2 mL min^{-1}. Despite the initial good conversions and excellent enantioselectivity (*e.g.*, 75% conversion and 95% ee), fast deactivation was observed, thus indicating that leaching of Pd complexes involving **L$_{11}$** was taking place.[68–71] This observation prompted us to modify the continuous flow protocol by simultaneously pumping small amounts of the Pd-precursor and auxiliary ligand together with the substrates through the packed bed reactor containing ligand PS-(*R*)-**L$_5$** (Scheme 4). This could be easily performed by simultaneous pumping of two different solutions. One of them contains the Pd-precursor in THF, and the other one contains both substrates ([**1a**] = 0.050 M, [**2a**] = 0.07 M) and the auxiliary ligand (5 mM). Both THF solutions were pumped simultaneously at 0.1 mL min^{-1} and mixed just before entering the packed bed reactor by using a T-mixer. Initially, we pumped a highly concentrated Pd precursor solution (2.5 mM) and when high levels of conversion were achieved, the initial Pd solution was replaced by a more diluted one (0.75 mM). Positively, after optimization, **3aa** was produced in good overall yield and enantioselectivity (up to 95% ee) for up to

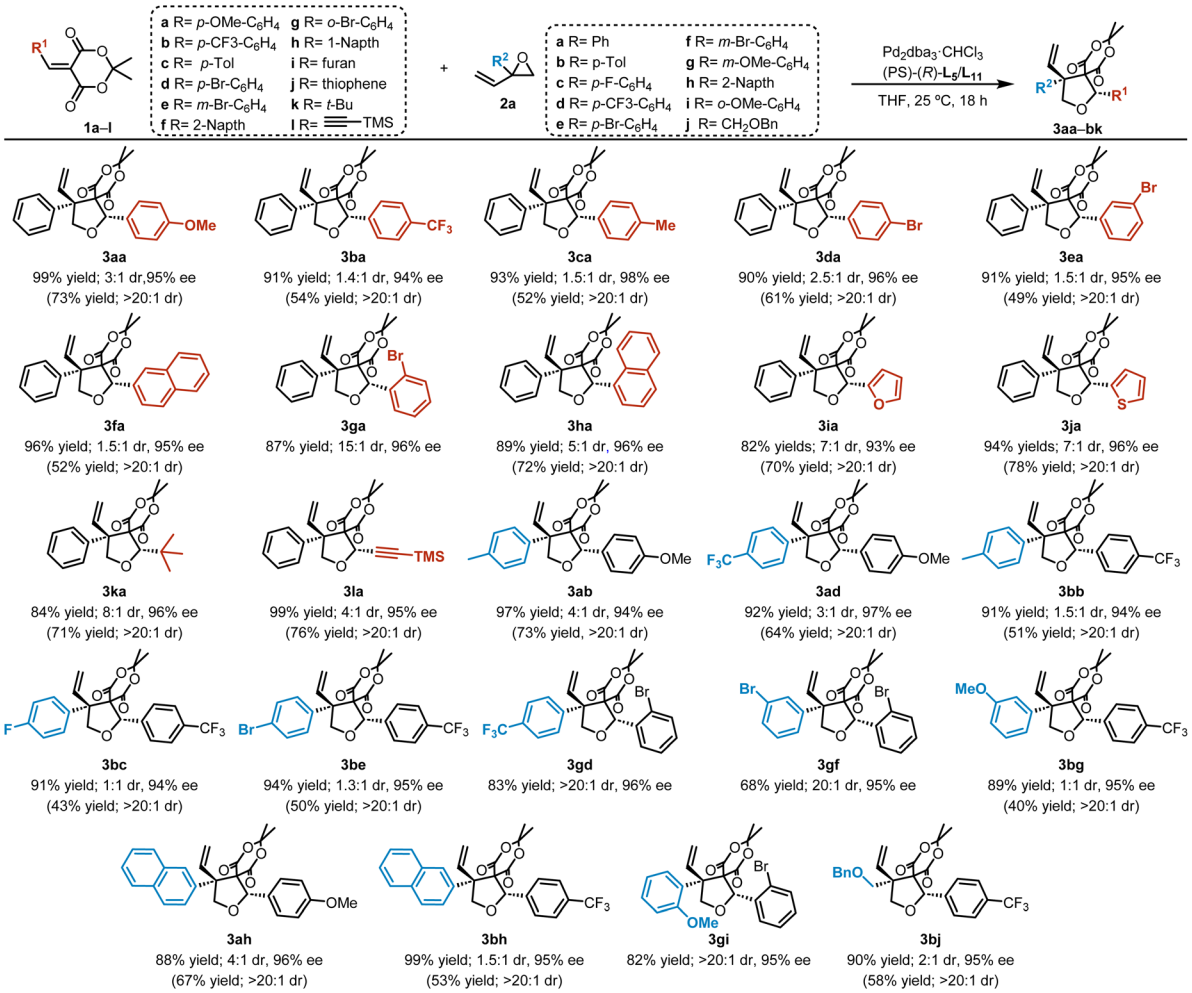

Scheme 3 Cycloaddition reactions using Pd(PS-(*R*)-L_5)L_{11} with several 5-(*R*-ylidene) substituted 2,2-dimethyl-1,3-dioxane-4,6-diones (in red) and vinylepoxides (in blue). The yields and diastereoselectivities for the major diastereomer after crystallization of selected final compounds are shown in parentheses.

3 h (Scheme 4). Interestingly, continuous addition of the auxiliary ligand and Pd-precursor did not diminish the high level of enantioselectivity, indicating that the reaction was happening solely at the resin, and there was no competition with the putative homogeneous complex bearing two homogeneous ligands.

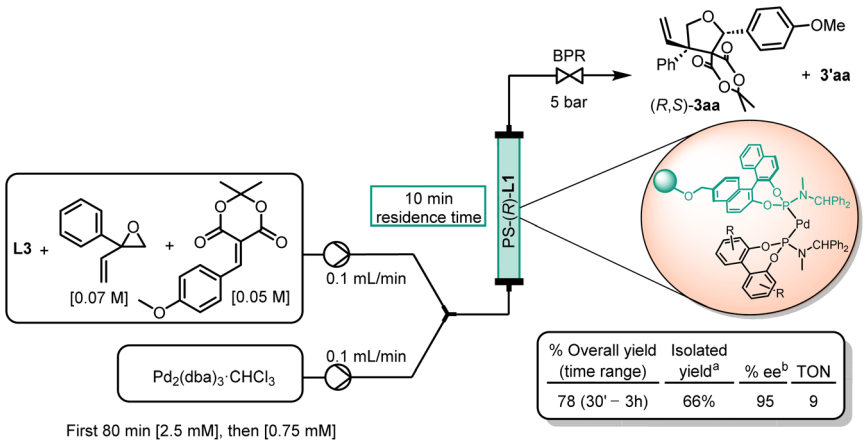

Scheme 4 Set up of the optimized continuous flow protocol to perform Pd-catalyzed asymmetric cycloadditions using well defined Pd(PS-(*R*)-L_5)L_{11} species. [a]Isolated as a 3 : 1 diastereomeric mixture. [b]Referred to **3aa** and determined by HPLC.

In summary, this heterogenous flow protocol, involving the cooperation of a homogeneous achiral ligand, that can be recovered after the reaction, enables to achieve high enantioselectivities in the preparation of **3** through simple and fast reactions (only 10 min of residence time). Moreover, it is a further confirmation that the reaction proceeds on the heterogeneous phase, and the observed catalytic activity has to be ascribed to well defined, immobilized Pd(PS-(*R*)-$\mathbf{L_5}$)$\mathbf{L_{11}}$ species and not to leached Pd species as in other Pd-catalytic systems reported in the literature.[72–76]

Conclusions

We have developed a new, simple methodology that allows the formation of well-defined highly enantioselective active species containing two different monodentate ligands coordinated at the same time to the metal center (ML^1L^2). This methodology takes advantage of covalently immobilizing one of the ligands onto a solid support with low functionalization, so that no homocombination of ligands ($ML^{Het}L^{Het}$) is possible, followed by its coordination to the metal and subsequently addition of a second different ligand in solution that can synergistically improve enantioselectivity. This methodology has been successfully applied in the Pd-catalyzed [3 + 2] spiroannulation for the synthesis of a wide range of tetrahydrofuran-fused spirocyclic Meldrum's acid derivatives (24 examples). The exclusive formation of the successful ML^1L^2-type species was achieved by combining a polystyrene supported chiral binaphthyl-based phosphoramidite with a cheap achiral biphenyl monophosphoramidite. Key to the success of this strategy have been (a) the use of a covalent immobilization to avoid leaching of the supported ligand (L^{Het}), (b) the immobilization of the ligand through a position far away from the catalytic center to avoid perturbation of the enantiodifferentiating transition states by the polymer backbone, and (c) the use of a low cross-linked polymer backbone with low functionalization, which allows fast mass transfer, approaching homogeneous conditions, while preventing the formation of $PdL^{Het}L^{Het}$ species. We have subsequently extended the use of this well-defined $PdL^{Het}L^{Hom}$ species to the spiroannulation in continuous flow. Positively, the selectivity of the cycloaddition reaction with the immobilized ligand is maintained when the system is operated in continuous flow mode. Leaching of Pd species during the continuous flow operation could be compensated by continuous addition of a solution of the Pd-precursor in THF. These flow experiments also demonstrated that Pd species in solution were not catalytically active, so that the catalytic performance of the spiroannulation reaction has to be ascribed to the heterogenous phase containing both types of monophosphoramidite ligands coordinated to Pd.

Preliminary results indicate that this approach to control ML^1L2 speciation can also be applied to enantioselective Pd-catalyzed allylic substitution reactions. Thus, the use of equimolar amounts of PS-(*R*)-$\mathbf{L_5}$ with achiral $\mathbf{L_{11}}$ provides higher enantioselectivity than that obtained under homogeneous conditions (62% *vs.* 40% ee) in the alkylation of 1,3-diphenylallyl acetate with dimethylmalonate (see SI for details). We are currently working on designing new catalytic systems of the general type $ML^{Het}L^{Hom}$ with increased metal–ligand ($M–L^{Het}$) stability, with the aim of minimizing metal leaching and thus transforming the present proof of principle into finely tunable processes, suitable for the long-standing operation in continuous flow.

Author contributions

The manuscript was written through contributions of all authors. All authors have given approval to the final version of the manuscript.

Conflicts of interest

There are no conflicts to declare.

Data availability

CCDC 2474009 (**3aa**) and 2474010 (**7**) contain the supplementary crystallographic data for this paper.[77a,b]

The data supporting this article have been included as part of the supplementary information (SI). Supplementary information: development and scope of the spiroannulation reaction, mechanistic investigations, experimental procedures for batch and flow spiroannulations, synthesis of immobilized ligand, synthesis of new ligands and substrates, post-modifications, characterization details and enantiomeric excess determination of products, copies of NMR spectra and of HPLC traces for ee determination of products, kinetic data and X-ray crystallographic data for compounds. See DOI: https://doi.org/10.1039/d6sc01392a.

Acknowledgements

This work was supported by grants from FEDER/Ministerio de Ciencia e Innovación (MICINN)/AEI (PID2022-139996NB-I00). Grant 2021SGR00163 funded by the Catalan Government are also gratefully acknowledged. J. F. also thanks Ministerio de Ciencia, Innovación y Universidades for FPU18/06352 fellowship. M. B. thanks to the "Ramón y Cajal" contract (RRYC-2023-045413-I) funded by MICIU/AEI/10.13039/501100011033 and ESF+.

Notes and references

1 *Privileged Chiral Ligands and Catalysts*, ed. Q.-L. Zhou, John Wiley& Sons Inc., New York, 2011.
2 *Chiral ligands. Evolution of ligand libraries for asymmetric catalysis*, ed. M. Diéguez, CRC Press, Boca Raton, 2021.
3 J. Margalef, M. Biosca, P. de la Cruz-Sánchez, J. Faiges, O. Pàmies and M. Diéguez, Evolution in heterodonor P-N, P-S and P-O chiral ligands for preparing efficient catalysts for asymmetric catalysis. From design to applications, *Coord. Chem. Rev.*, 2021, **446**, 214120.
4 T. P. Dang and H. B. Kagan, The asymmetric synthesis of hydratropic acid and amino-acids by homogeneous

catalytic hydrogenation, *J. Chem. Soc. Chem. Commun.*, 1971, 481.
5 F. Guillen and J.-C. Fiaud, Enantiomerically pure 1, 2, 5-triphenylphospholane through the synthesis and resolution of the chiral trans-(2,5)-diphenylphospholanic acid, *Tetrahedron Lett.*, 1999, **40**, 2939–2942.
6 C. Claver, E. Fernandez, A. Gillon, K. Heslop, D. J. Hyett, A. Martorell, A. G. Orpen and P. G. Pringle, Biarylphosphonites: a class of monodentate phosphorus(III) ligands that outperform their chelating analogues in asymmetric hydrogenation catalysis, *Chem. Commun.*, 2000, 961–962.
7 M. T. Reetz and T. Sell, Rhodium-catalyzed enantioselective hydrogenation using chiral monophosphonite ligands, *Tetrahedron Lett.*, 2000, **41**, 6333–6336.
8 M. T. Reetz and G. Mehler, Highly Enantioselective Rh-Catalyzed Hydrogenation Reactions Based on Chiral Monophosphite Ligands, *Angew. Chem., Int. Ed.*, 2000, **39**, 3889–3890.
9 G. Franció, F. Faraone and W. Leitner, Asymmetric catalysis with chiral phosphane/phosphoramidite ligands derived from quinoline (QUINAPHOS), *Angew. Chem., Int. Ed.*, 2000, **39**, 1428–1430.
10 M. van den Berg, A. J. Minnaard, E. P. Schudde, J. van Esch, A. H. M. de Vries, J. G. de Vries and B. L. Feringa, Highly enantioselective rhodium-catalyzed hydrogenation with monodentate ligands, *J. Am. Chem. Soc.*, 2000, **122**, 11539–11540.
11 For a review illustrating the succesful use of monodentate phosphorus ligands, see: W. Fu and W. Tang, Chiral monophosphorus ligands for asymmetric catalytic reactions, *ACS Catal.*, 2016, **6**, 4814–4858.
12 Several metal catalytic asymmetric reactions have benefited from the use of nonsymmetrical bidentate P–P′ ligands since both functionalities can be independently boosted. See for example: A. Pfaltz and W. J. Drury III, Design of chiral ligands for asymmetric catalysis: From C2-symmetric P,P- and N,N-ligands to sterically and electronically nonsymmetrical P,N-ligands, *Proc. Natl. Acad. Sci. U. S. A.*, 2004, **101**, 5723–5726.
13 M. T. Reetz, T. Sell, A. Meiswinkel and G. Mehler, A New Principle in Combinatorial Asymmetric Transition-Metal Catalysis: Mixtures of Chiral Monodentate P Ligands, *Angew. Chem., Int. Ed.*, 2003, **42**, 790–793.
14 M. T. Reetz and G. Mehler, Mixtures of chiral and achiral monodentate ligands in asymmetric Rh-catalyzed olefin hydrogenation: reversal of enantioselectivity, *Tetrahedron Lett.*, 2003, **44**, 4593–4596.
15 M. T. Reetz, Combinatorial Transition-Metal Catalysis: Mixing Monodentate Ligands to Control Enantio-, Diastereo-, and Regioselectivity, *Angew. Chem., Int. Ed.*, 2008, **47**, 2556–2588.
16 C. Rodríguez-Escrich and M. A. Pericàs, Organocatalysis on Tap: Enantioselective Continuous Flow Processes Mediated by Solid-Supported Chiral Organocatalysts, *Eur. J. Org Chem.*, 2015, 1173–1188.
17 C. Rodriguez-Escrich and M. A. Pericàs, Catalytic Enantioselective Flow Processes with Solid-Supported Chiral Catalysts, *Chem. Rec.*, 2019, **19**, 1872–1890.
18 X. Fan, C. Rodríguez-Escrich, S. Sayalero and M. A. Pericàs, Paraldehyde as an Acetaldehyde Precursor in Asymmetric Michael Reactions Promoted by Site-isolated Incompatible Catalysts, *Chem.–Eur. J.*, 2013, **19**, 10814–10817.
19 X. Fan, C. Rodríguez-Escrich, S. Wang, S. Sayalero and M. A. Pericàs, Highly Enantioselective Cross-Aldol Reactions of Acetaldehyde Mediated by a Dual Catalytic System Operating under Site Isolation, *Chem.–Eur. J.*, 2014, **20**, 13089–13093.
20 P. Borah, M. Fianchini and M. A. Pericàs, Assessing the Role of Site Isolation and Compartmentalization in Packed Bed Flow Reactors for Processes Involving Wolf-and-Lamb Scenarios, *ACS Catal.*, 2021, **11**, 6234–6242.
21 L. Capaldo, W. Zhenghui and T. Noël, A field guide to flow chemistry for synthetic organic chemists, *Chem. Sci.*, 2023, **14**, 4230–4247.
22 F. Parveen, N. Watson, A. M. Scholes and A. G. Slater, Continuous flow as an enabling technology for sustainable supramolecular chemistry, *Curr. Opin. Green Sustainable Chem.*, 2024, **48**, 100935.
23 M. Lautens, W. Klute and W. Tam, Transition Metal-Mediated Cycloaddition Reactions, *Chem. Rev.*, 1996, **96**, 49–92.
24 L. Yet, Metal-Mediated Synthesis of Medium-Sized Rings, *Chem. Rev.*, 2000, **100**, 2963–3008.
25 X. Xu and M. P. Doyle, The [3 + 3]-Cycloaddition Alternative for Heterocycle Syntheses: Catalytically Generated Metalloenolcarbenes as Dipolar Adducts, *Acc. Chem. Res.*, 2014, **47**, 1396–1405.
26 T. Hashimoto and K. Maruoka, Recent Advances of Catalytic Asymmetric 1,3-Dipolar Cycloadditions, *Chem. Rev.*, 2015, **115**, 5366–5412.
27 B. M. Trost, Z. Zuo and J. E. Schultz, Transition-Metal-Catalyzed Cycloaddition Reactions to Access Seven-Membered Rings, *Chem.–Eur. J.*, 2020, **26**, 15354–15377.
28 P. de la Cruz-Sánchez and O. Pàmies, Metal-π-Allyl Mediated Asymmetric Cycloaddition Reactions, *Adv. Catal.*, 2021, **69**, 103–180.
29 J. He, J. Ling and P. Chiu, Vinyl Epoxides in Organic Synthesis, *Chem. Rev.*, 2014, **114**, 8037–8128.
30 D. W. B. Allen, C. P. Lakeland and J. P. A. Harrity, Utilizing Palladium-Stabilized Zwitterions for the Construction of N-Heterocycles, *Chem.–Eur. J.*, 2017, **23**, 13830–13857.
31 N. De and E. J. Yoo, Recent Advances in the Catalytic Cycloaddition of 1,n-Dipoles, *ACS Catal.*, 2018, **8**, 48–58.
32 Y. Liu, J. Oble, A. Pradal and G. Poli, Catalytic Domino Annulations through η^3-Allylpalladium Chemistry: A Never-Ending Story, *Eur. J. Inorg. Chem.*, 2020, 942–961.
33 B. M. Trost and G. Mata, Forging Odd-Membered Rings: Palladium-Catalyzed Asymmetric Cycloadditions of Trimethylenemethane, *Acc. Chem. Res.*, 2020, **53**, 1293–1305.
34 J. Wang, S. A. Blaszczyk, X. Li and W. Tang, Transition Metal-Catalyzed Selective Carbon–Carbon Bond Cleavage of

Vinylcyclopropanes in Cycloaddition Reactions, *Chem. Rev.*, 2021, **121**, 110–139.

35 C. Yang, Z.-X. Yang, C.-H. Ding, B. Xu and X.-L. Hou, Development of Dipolarophiles for Catalytic Asymmetric Cycloadditions through Pd-π-Allyl Zwitterions, *Chem. Rec.*, 2021, **21**, 1442–1454.

36 Even though the use of monophosphoramidite ligands for the enantioselective Pd-catalyzed [3 + 2] cycloaddition has been previously disclosed, there are examples for which the use of Pd/monophosphoramidite catalyst precursors are not active. See for example: J.-J. Suo, J. Du, Q.-R. Liu, D. Chen, C.-H. Ding, Qi. Peng and X.-L. Hou, Highly Diastereo- and Enantioselective Palladium-Catalyzed [3 + 2] Cycloaddition of Vinyl Epoxides and α,β-Unsaturated Ketones, *Org. Lett.*, 2017, **19**, 6658.

37 Spirocycles have a unique balance between structural rigidity and individual ring-related conformational flexibility, which for instance in drug discovery are key to overcome many liabilities of typical drug scaffolds based on flat (hetero)aromatics.

38 Y. Zheng, C. M. Tice and S. B. Singh, The Use of Spirocyclic Scaffolds in Drug Discovery, *Bioorg. Med. Chem. Lett.*, 2014, **24**, 3673–3682.

39 E. M. Carreira and T. C. Fessard, Four-Membered Ring-Containing Spirocycles: Synthetic Strategies and Opportunities, *Chem. Rev.*, 2014, **114**, 8257–8322.

40 E. Chupakhin, O. Babich, A. Prosekov, L. Asyakina and M. Krasavin, Spirocyclic Motifs in Natural Products, *Molecules*, 2019, **24**, 4165.

41 P. Yadav, R. Pratap and V. Ji Ram, Natural and Synthetic Spirobutenolides and Spirobutyrolactones, *Asian J. Org. Chem.*, 2020, **9**, 1377–1409.

42 K. Acosta-Quiroga, C. Rojas-Peña, L. S. Nerio, M. Gutiérrez and E. Polo-Cuadrado, Spirocyclic Derivatives as Antioxidants: a Review, *RSC Adv.*, 2021, **11**, 21926–21954.

43 To the best of our knowledge the use of Meldrum's acid derivatives for the formation of spirocyclic compounds *via* Pd-catalyzed asymmetric [3 + 2] cycloaddition have not been reported. A single racemic example can be found in J.-G. Shim and Y. Yamamoto, Palladium-Catalyzed Regioselective [3 + 2] Cycloaddition of Vinylic Oxiranes with Activated Olefins. A Facile Synthesis of Tetrahydrofuran Derivatives, *J. Org. Chem.*, 1998, **63**, 3067–3071.

44 L. Panizzi, L. Mangoni and M. Belardini, The Structure of Grindelic Acid, a New Diterpene Acid, *Tetrahedron Lett.*, 1961, **2**, 376–381.

45 F. J. Schmitz, F. J. McDonald and D. J. Vanderah, Marine Natural Products: Sesquiterpene Alcohols and Ethers from the Sea Hare Aplysia Dactylomela, *J. Org. Chem.*, 1978, **43**, 4220–4225.

46 E. Lee, D. S. Lee, Y. W. Choi and K. H. Lee, Stereoselective Reduction of α-Iodospirolactones. Total Synthesis of (±)-Liguloxide, *Tetrahedron Lett.*, 1992, **33**, 6673–6676.

47 Y. K. Booth, W. Kitching and J. J. De Voss, Biosynthesis of Insect Spiroacetals, *Nat. Prod. Rep.*, 2009, **26**, 490–525.

48 A. Miyawaki, D. Kikuchi, M. Niki, Y. Manabe, M. Kanematsu, H. Yokoe, M. Yoshida and K. Shishido, Total Synthesis of Natural Enantiomers of Heliespirones A and C via the Diastereoselective Intramolecular Hosomi-Sakurai Reaction, *J. Org. Chem.*, 2012, **77**, 8231–8243.

49 D. R. Bhatia, P. Dhar, V. Mutalik, S. K. Deshmukh, S. A. Verekar, D. C. Desai, R. Kshirsagar, P. Thiagarajan and V. Agarwal, Anticancer Activity of Ophiobolin A, Isolated from the Endophytic Fungus Bipolaris Setariae, *Nat. Prod. Res.*, 2016, **30**, 1455–1458.

50 D. Q. Thach, Z. G. Brill, H. K. Grover, K. V. Esguerra, J. K. Thompson and T. J. Maimone, Total Synthesis of (+)-6-epi- Ophiobolin A, *Angew. Chem., Int. Ed.*, 2020, **59**, 1532–1536.

51 C. Ma, Y. Huang and Y. Zhao, Stereoselective 1,6-Conjugate Addition/Annulation of para-Quinone Methides with Vinyl Epoxides/Cyclopropanes, *ACS Catal.*, 2016, **6**, 6408–6412 (dr's: 5/1–>20/1 and ee's: 74–>99%).

52 J.-A. Xiao, Y.-C. Li, Z.-J. Luo, X.-L. Cheng, Z.-X. Deng, W.-Q. Chen, W. Su and H. Yang, Construction of Bispirooxindole Heterocycles via Palladium-Catalyzed Ring-Opening Formal [3+ 2]-Cycloaddition of Spirovinylcyclopropyl Oxindole and 3-Oxindole and 3-Oxindole Derivatives, *J. Org. Chem.*, 2019, **84**, 2297–2306 (dr: 5/1 and 71% ee).

53 J. Wang, L. Zhao, Q. Rong, R. Lv, Y. Lu, X. Pan, L. Zhao and L. Hu, Asymmetric synthesis of 3, 3′-tetrahydrofuryl spirooxindoles via palladium-catalyzed [3+ 2] cycloadditions of methyleneindolinones with vinylethylene carbonates, *Org. Lett.*, 2020, **22**, 5833–5838 (>20/1 dr's and ee's: 45–99%).

54 H. Zhang, X. Gao, F. Jiang, W. Shi, W. Wang, Y. Wu, C. Zhang, X. Shi and H. Guo, Palladium-Catalyzed Asymmetric [3+2] Cycloaddition of Vinylethylene Carbonates with 2-Arylidene-1,3-Indandiones: Synthesis of Tetrahydrofuran-Fused Spirocyclic 1,3-Indandiones, *Eur. J. Org Chem.*, 2020, 4801–4804 (dr's: 1/1–4/1 and ee's: 75–99% at 0 °C).

55 H. J. Jeon, S. M. Park, Y. M. Lee and S.-G. Lee, Divergent Asymmetric Synthesis of Chiral Spiroheterocycles through Pd-Catalyzed Enantio- and Diastereoselective [3 + 2] Spiroannulation, *Org. Lett.*, 2022, **24**, 9189–9193 (dr's: 1.1/1–16/1 and ee's: 62–99% at 45 °C).

56 E. Pair, T. Cadart, V. Levacher and J.-F. Brière, Meldrum's Acid: A Useful Platform in Asymmetric Organocatalysis, *ChemCatChem*, 2016, **8**, 1882–1890.

57 S. N. A. Bukhari, M. A. Abdelgawad, N. Ahmed, M. W. Amjad, M. A. Hussain, M. A. Elsherif, H. Ejaz, N. H. Alotaibi, I. Filipović and N. Janković, Synthesis, Characterization, and Biological Evaluation of Meldrum's Acid Derivatives: Dual Activity and Molecular Docking Study, *Pharmaceuticals*, 2023, **16**, 281.

58 F. Brosge, P. Singh, F. Almqvist and C. Bolm, Selected Applications of Meldrum's Acid – a Tutorial, *Org. Biomol. Chem.*, 2021, **19**, 5014–5027.

59 J. Burés, Variable Time Normalization Analysis: General Graphical Elucidation of Reaction Orders from

Concentration Profiles, *Angew. Chem., Int. Ed.*, 2016, **55**, 16318–16321.

60 J. Burés, A Simple Graphical Method to Determine the Order in Catalyst, *Angew. Chem., Int. Ed.*, 2016, **55**, 2028–2031.

61 C. D.-T. Nielsen and J. Burés, Visual kinetic analysis, *Chem. Sci.*, 2019, **10**, 348–353.

62 C. Jaramillo-Ferrer, G. Hutchinson and J. Burés, Mechanistic interpretation of orders in catalyst greater than one, *Nat. Rev.*, 2023, **7**, 26–34.

63 H. Eyring, The Activated Complex in Chemical Reactions, *J. Chem. Phys.*, 1935, **3**, 107–115.

64 D. Jayaprakash and H. Sasai, Synthesis and catalytic applications of soluble polymer-supported BINOL, *Tetrahedron: Asymmetry*, 2001, **12**, 2589–2595.

65 A. Vidal-Ferran, N. Bampos, A. Moyano, M. A. Pericàs, A. Riera and J. K. M. Sanders, High catalytic activity of chiral amino alcohol ligands anchored to polystyrene resins, *J. Org. Chem.*, 1998, **63**, 6309–6318.

66 M. Diéguez, O. Pàmies and C. Moberg, Self-Adaptable Tropos Catalysts, *Acc. Chem. Res.*, 2021, **54**, 3252–3263.

67 The higher enantioselectivity observed with $\mathbf{L_{11}}$ compared to that obtained with $\mathbf{L_{10}}$ can be explained either by the steric effect of the *tert*-butyl moieties at the *ortho* positions of the biphenyl moiety, by a slightly different dihedral angle of the biphenyl group in $\mathbf{L_{10}}$/$\mathbf{L_{11}}$, or by a combination of both factors.

68 Note that during the reaction, the palladium species gets oxidized to Pd(II), which are known to favour the Pd-leaching.

69 B. Gutmann, D. Cantillo and C. O. Kappe, Continuous-Flow Technology—A Tool for the Safe Manufacturing of Active Pharmaceutical Ingredients, *Angew. Chem., Int. Ed.*, 2015, **54**, 6688–6728.

70 D. Cantillo and C. O. Kappe, Immobilized Transition Metals as Catalysts for Cross-Couplings in Continuous Flow—A Critical Assessment of the Reaction Mechanism and Metal Leaching, *ChemCatChem*, 2014, **6**, 3286–3305.

71 R. Greco, W. Goessler, D. Cantillo and C. O Kappe, Benchmarking immobilized di-and triarylphosphine palladium catalysts for continuous-flow cross-coupling reactions: efficiency, durability, and metal leaching studies, *ACS Catal.*, 2015, **5**, 1303–1312.

72 N. T. S. Phan, M. Van Der Sluys and C. W. Jones, On the Nature of the Active Species in Palladium Catalyzed Mizoroki–Heck and Suzuki–Miyaura Couplings–Homogeneous or Heterogeneous Catalysis, a Critical Review, *Adv. Synth. Catal.*, 2006, **348**, 609–679.

73 A. F. Shmidt and L. V. Mametova, Main Features of Catalysis in the Styrene Phenylation Reaction, *Kinet. Catal.*, 1996, **37**, 406–408.

74 R. G. Heidenreich, J. G. E. Krauter, J. Pietsch and K. Kohler, Control of Pd Leaching in Heck Reactions of Bromoarenes Catalyzed by Pd Supported on Activated Carbon, *J. Mol. Catal. A: Chem.*, 2002, **182**, 499–509.

75 K. Kohler, R. G. J. Heidenreich, G. E. Krauter and M. Pietsch, Highly Active Palladium/Activated Carbon Catalysts for Heck Reactions: Correlation of Activity, Catalyst Properties, and Pd Leaching, *Chem.–Eur. J.*, 2002, **8**, 622–631.

76 R. K. Arvela, N. E. Leadbeater, M. S. Sangi, V. A. Williams, P. Granados and R. D. A. Singer, Reassessment of the Transition-Metal Free Suzuki-Type Coupling Methodology, *J. Org. Chem.*, 2005, **70**, 161–168.

77 (*a*) CCDC 2474009: Experimental Crystal Structure Determination, 2026, DOI: 10.5517/ccdc.csd.cc2p1drx.; (*b*) CCDC 2474010: Experimental Crystal Structure Determination, 2026, DOI: 10.5517/ccdc.csd.cc2p1dsy.